

Silver oligomer and single fullerene electronic properties revealed by a scanning tunnelling microscope

H. Jensen, J. Kröger^a, N. Néel, and R. Berndt

Institut für Experimentelle und Angewandte Physik, Christian-Albrechts-Universität zu Kiel, 24098 Kiel, Germany

Received 24 January 2007 / Received in final form 11 April 2007

Published online 16 May 2007 – © EDP Sciences, Società Italiana di Fisica, Springer-Verlag 2007

Abstract. Clusters on surfaces have been investigated with low-temperature scanning tunnelling microscopy and spectroscopy. Constant current spectra acquired on Ag oligomers and one-dimensional chains on a Ag(111) reveal a single resonance peak whose energy shifts towards the Fermi level with increasing cluster size. Next, controlled and reproducible contact between a STM tip and a C₆₀ molecule adsorbed on Cu(100) is reported. The transition from tunnelling to contact is discussed in terms of local heating of the tip-molecule junction.

PACS. 73.22.-f Electronic structure of nanoscale materials: clusters, nanoparticles, nanotubes, and nanocrystals – 61.48.+c Fullerenes and fullerene-related materials – 68.37.-d Microscopy of surfaces, interfaces, and thin films – 68.37.Ef Scanning tunneling microscopy

1 Introduction

Scanning tunnelling microscopy (STM) and related techniques have been extensively used in manipulating and characterizing clusters adsorbed on conducting surfaces. A significant benefit is the spatial resolution that eliminates ensemble effects, enables to directly control cluster size, geometry and adsorption environment, and ultimately assemble clusters in situ from their constituent atoms. The extent to which the electronic structures of adsorbed clusters and substrate interact has been a focus of considerable interest. In this context, the noble metal (111) faces have been prominently employed as they provide quasi-two-dimensional electronic states localised to the surface, with a nearly free-electron like dispersion, readily accessible by surface analysis techniques. While the electronic structure of an adsorbed cluster has been shown to significantly depend on cluster size and shape [1–6], the interaction with the substrate can be probed by studying variations in the properties of the surface state.

The scanning tunnelling microscope appears to be an ideal tool to study the conductance of single atoms or clusters in detail. The structure to be analysed can be imaged in direct space with atomic precision prior to and after taking conductance data. Thus, specific locations of the structure can be addressed and possible modifications can be easily detected. Another advantage of STM is the possibility to characterize to some extent the status of the second electrode, the microscope tip, by recording conductance data on clean metal areas. Indeed, scanning probe

techniques have been used to form point contacts between the tip and a metal surface whose quantized conductance was then investigated during forming and stretching of the contact [7–9]. Taking advantage of the imaging capability of STM recent experiments on individual adsorbed atoms (adatom) [10–13] and on C₆₀ [14] showed that contacts can be formed reproducibly without structural change of tip or sample.

In this article we present a low-temperature scanning tunnelling spectroscopy study of Ag oligomers and one-dimensional Ag chains adsorbed on an Ag(111) substrate. Moreover, we address the controlled and reproducible contact between the tip of the microscope and C₆₀ adsorbed on a Cu(100) surface.

2 Experiment

Measurements were performed using a custom-built low-temperature ultra-high vacuum scanning tunnelling microscope operated at 7 K and at a base pressure of better than 10^{−9} Pa. Surfaces of Ag(111) and Cu(100) as well as electrochemically etched tungsten tips were prepared by argon ion bombardment and annealing. Controlled indentations of the tip into substrate material was repeated until adatoms appeared with nearly circular shape in constant-current images and spectra of the differential conductivity (dI/dV) did not contain electronic structure of the tip. As a consequence of this tip preparation technique the apex of the tungsten tip was most probably covered with several layers of the corresponding substrate material. Single silver atoms were deposited onto Ag(111) by

^a e-mail: kroeger@physik.uni-kiel.de

controlled tip-surface contacts as previously described for silver and copper atoms in reference [11].

To prepare Ag oligomers, the Ag-coated tip is initially positioned atop a clean terrace of the Ag(111) surface. Starting from a tunnelling current of $1\ \mu\text{A}$ at a sample bias voltage of $100\ \text{mV}$, the tip is ramped towards the surface at a speed of $\approx 3\ \text{\AA s}^{-1}$ until, after approximately 1 to $2\ \text{\AA}$ of tip displacement, a discontinuity in the $I(z)$ characteristic is observed, indicating the drop-off of tip material onto the surface. In a series of these preparations, the size of the deposited objects is statistically distributed [15]. In the majority of cases a single Ag atom is adsorbed, appearing as a circular object of $0.3\ \text{\AA}$ height and $7.5\ \text{\AA}$ full width at half maximum (FWHM). Also frequently observed are Ag_2 dimers and Ag_3 trimers. The number of atoms within a cluster was inferred from the cluster size in STM images. Dimers are imaged as protrusions of $0.5\ \text{\AA}$ height and $10\ \text{\AA}$ FWHM. We suggest intracell diffusion as the mechanism leading to the circular appearance of the dimers. A similar effect is seen in the Cu_2 dimer on Cu(111) that also appears as a circular object at $T = 7\ \text{K}$ due to the movement of the two constituent atoms within a local hexagonal diffusion cell [4]. The trimer appears as a round object of $0.6\ \text{\AA}$ height and $11\ \text{\AA}$ FWHM, from which we conclude that the cluster is of compact triangular geometry. While rotational diffusion of the whole trimer — leaving its compact shape intact — cannot be ruled out from the topographic data alone, simulations for Cu_3 on Cu(111) suggest a stable configuration at temperatures below $21\ \text{K}$ [4]. We expect this to be similar for Ag_3 on Ag(111). Occasionally, bigger, irregularly formed clusters are dropped from the tip.

Indenting the tip by a larger distance of about 30 to $50\ \text{\AA}$ will locally induce an area of severe surface disorder. From this, artificial straight step edges are created. Owing to the hexagonal Ag(111) substrate lattice, these steps extend into the six crystallographic directions. In the periphery of the indentation sites, a variety of local surface dislocations may occur. These include straight step edges [16], as well as monatomically deep protrusions and depressions of triangular shape [17]. Additionally, linear Ag chains and trenches appear, their widths frequently as low as a single atomic row. These structures are remarkable models of a linear cluster due to their flawless linear geometry over distances often exceeding $1000\ \text{\AA}$ (see, for instance, the scattering of the Ag(111) surface state at a linear monatomically wide Ag chain presented in Fig. 1).

In the experiment, we performed differential conductivity spectroscopy on top of Ag_1 , Ag_2 and triangular Ag_3 adsorbates, as well as on a monatomic chain, all of these having been fabricated using the above-mentioned technique. Spectra were acquired at positive sample voltages ranging from 1 to $3.5\ \text{V}$, thereby probing the local density of unoccupied states. We notice that, due to the large variation in tunnelling current in the voltage range, we employ constant current spectroscopy, varying the tip height to maintain a constant current. While this complicates a quantitative evaluation of the local density of states the general features of a spectrum are retained.

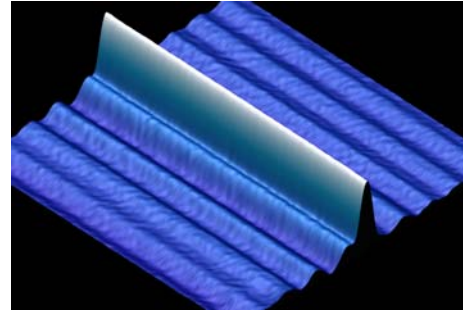


Fig. 1. Pseudo-three-dimensional representation of a STM image acquired at $V = 100\ \text{mV}$ and $I = 0.2\ \text{nA}$ (size: $170\ \text{\AA} \times 170\ \text{\AA}$). The Ag(111) Shockley-type surface state is scattered from a monatomically wide chain of silver atoms (structure with largest apparent height) giving rise to a standing wave pattern in front of and behind the chain.

C_{60} was evaporated from a tantalum crucible while keeping the residual gas pressure below $5 \times 10^{-8}\ \text{Pa}$. An ordered C_{60} superstructure was obtained by deposition onto the clean surface at room temperature and subsequent annealing to $500\ \text{K}$. Deposition rates were calibrated with a quartz microbalance to be $\approx 1\ \text{ML min}^{-1}$. We define a monolayer (ML) as one C_{60} molecule per sixteen copper atoms.

Prior to acquiring current-versus-displacement curves at a chosen surface location the tip-sample distance was fixed by opening the feedback loop of the microscope at a given current and sample voltage. Then the tip was approached towards the surface by $\approx 45\ \text{\AA s}^{-1}$ and simultaneously the current was acquired. For conductance measurements tunnelling currents of the order of $10\ \mu\text{A}$ are involved. Even at these elevated currents the voltage drop at the current-to-voltage converter is negligible. Conductances, $G = I/V$, can therefore be calculated using the sample voltage, V , which is applied to the tunnelling and contact junction.

3 Results and discussion

3.1 Silver oligomers

Constant current spectra on the Ag clusters have been acquired at a tunnelling current of $200\ \text{pA}$ and are displayed in Figure 2. It has been verified that spectroscopy of the clean substrate reveals a featureless background in the relevant energy range. Field emission resonances, for instance, start to set in at sample voltages as high as $\approx 4.5\ \text{V}$. On a single Ag atom, a single broad peak is observed at an energy of $2.95\ \text{eV}$ above the Fermi level E_F , marking a significant increase in the conductance of the tunnelling junction. We attribute this increase to the possibility of tunnelling through an unoccupied quasiautomatic resonance in this energy range [3]. The resulting peak resembles a Gaussian. We determine the peak height by subtracting a linear background connecting the tails of the Gaussian. From this, we obtain the two energies where the spectrum intersects an amplitude of half the peak value. The

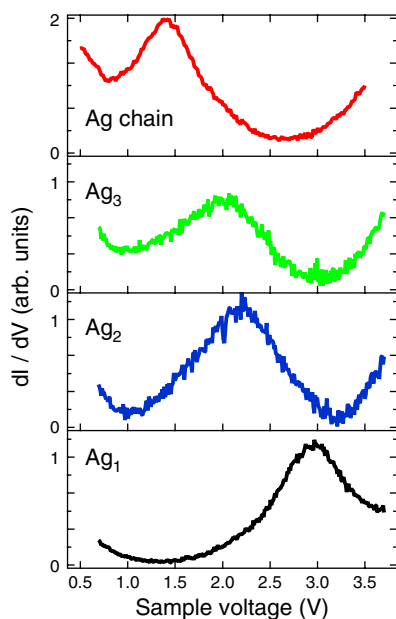


Fig. 2. (Color online) Constant current dI/dV spectra taken on top of Ag_1 , Ag_2 , Ag_3 and a monatomically wide Ag chain (bottom to top) adsorbed on Ag(111) at a current $I = 200$ pA.

distance between these energies is designated the FWHM and is determined to be 0.65 eV.

On the Ag_2 dimer we detect a peak at 2.25 eV, with an increased FWHM of 1.0 eV. The circular appearance of the dimer indicates that the constituent atoms are mobile but confined within their hexagonal substrate unit cell [18]. As this motion occurs at a speed beyond the time resolution of data acquisition, the appearance of the dimer is smoothed out. The spectra of the individual dimer configurations are averaged into a broadened peak. Similar intracell motion has been reported in the Cu_2 dimer on Cu(111), at a temperature of 7 K [4]. The dimensions of the trimer (see experiment section) lead to the conclusion that the cluster is of compact triangular geometry. Occasionally, bigger, irregularly formed clusters are dropped from the tip. It has previously been reported that, in a system where various types of dimers coexist whose atoms are situated on different combinations of lattice sites, spectroscopy reveals a variation of resonance energy with interatomic distance [3].

The Ag_3 trimer shows a peak of 0.8 eV FWHM whose energy position is shifted further downward 1.95 eV. Finally, on the monatomic Ag chain, we detect a peak at 1.4 eV, with a FWHM of 0.6 eV. We exclude the possibility of the resonances being related to field emission resonances as it has been verified that the lowest pertaining peak appears in spectroscopy beyond 4 eV, both on the clean surface and on the monatomic chain. All spectra were acquired on the centre of the clusters, i.e., at the position of maximum apparent height. Discernible qualitative changes of spectra by modifying the position of data acquisition were not observed. With the tips used in the present experiments atomic resolution of the sub-

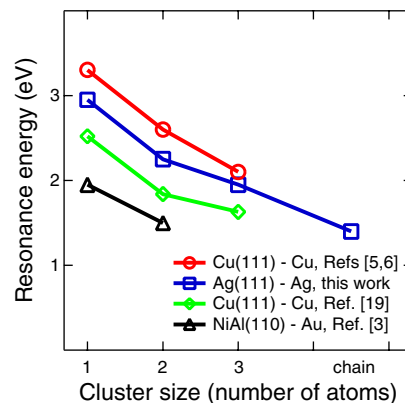


Fig. 3. (Color online) Comparison of lowest resonance peak position as a function of cluster size. Circles present data taken from reference [5] (atom, dimer) and reference [6] (trimer); squares denote data from present experiments; lozenges are data taken from reference [19]; triangles depict data from reference [3].

strate was not achieved. Therefore the adsorption site of Ag atoms remains unknown. However, spectra acquired on many atoms did not exhibit different spectroscopic signatures, which may hint at the equivalence of face-centred cubic (fcc) and hexagonal close-packed (hcp) adsorption sites or at Ag atoms occupying either the fcc or the hcp sites.

For comparison, a study of linear Cu oligomers on Cu(111) has demonstrated a similar behaviour, with the energy position of the lowest and most discernible resonance decreasing from 3.3 eV (0.6 eV FWHM) for the single atom to 2.6 eV and 2.0 eV for the Cu_2 and Cu_3 clusters, respectively [5]. However, it must be noted that the Cu_3 cluster is of linear shape, instead of the triangular shape observed for the Ag_3 cluster. Spectroscopy of a close-packed, triangular Cu_3 trimer yields a spectrum with a single resonance at 2.1 eV [6]. Also, broadening of the Cu_2 resonance to a FWHM of 0.9 eV by dimeric intracell diffusion is observed.

An ab initio calculation of $Cu_n/Cu(111)$ reveals a similar trend of decreasing resonance energy with cluster size, from 2.52 eV for the atom, to 1.84 eV for the dimer and 1.63 eV for a linear trimer [19].

Additionally, a study of Au oligomers on NiAl(110) shows a spectrum with a resonance at 1.95 eV for the single atom that splits symmetrically into a pair of resonances for the Au_2 dimer by an energy that depends on the distance of the constituent atoms [3]. For the closest observed distance, the lower peak is situated at 1.5 eV.

A compilation of the energy positions of the relevant spectral resonances for these studies are shown in Figure 3. In all these cases an increase in cluster size leads to a downward shift of lowest observed resonance energy.

3.2 Contact to a single C_{60}

In this paragraph we discuss the transition region from tunnelling to contact between the tip of a scanning

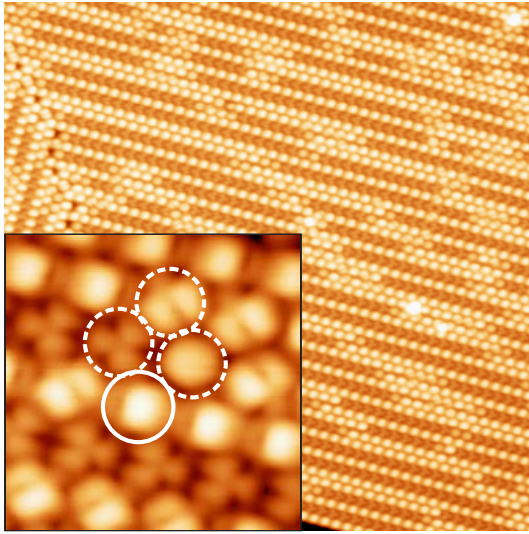


Fig. 4. Constant-current STM image of a C_{60} island adsorbed on Cu(100) (voltage: $V = 1.5$ V, current: $I = 1$ nA, size: $400 \text{ \AA} \times 400 \text{ \AA}$). Molecule chains appear as dark and bright lines due to adsorption-induced substrate surface missing row reconstruction. Inset: close-up view revealing sub-molecular details as predominantly induced by the spatial distribution of the LUMO+1-related density of states. Four molecular orientations are depicted by circles (size: $75 \text{ \AA} \times 75 \text{ \AA}$).

tunnelling microscope and an individual C_{60} molecule adsorbed on Cu(100). As revealed by the constant-current STM image shown in Figure 4, C_{60} adsorption on Cu(100) in the sub-monolayer coverage regime induces a missing-row reconstruction of the substrate surface [20]. Chain-like structures with different contrast are attributed to linear molecule assemblies adsorbed in missing copper rows. While chains with lower contrast represent molecules occupying sites within a double missing row, chains with higher contrast are assigned to molecules adsorbed in a single missing row. Similar to Ag(100)- C_{60} [21] we observe four molecular orientations on Cu(100) (see inset of Fig. 4). The STM image of the inset of Figure 4 was acquired at a sample voltage of 1.5 V which corresponds to the energy of the second-to-lowest unoccupied molecular orbital (LUMO+1). As a consequence, sub-molecular contrast is dominated by the spatial distribution of the LUMO+1 density of states.

Figure 5 displays a current-versus-displacement curve as acquired upon tip approach towards the centre of a C_{60} molecule of the 5:6 type (see the molecule encircled by a full line in the inset of Fig. 4). This molecule is oriented such as to exhibit a carbon-carbon bond between a carbon pentagon and a carbon hexagon at the top. Displacement $\Delta z = 0$ corresponds to the tip height above the molecule which is fixed by opening the feedback loop (300 mV, 3 nA) prior to acquiring the current curve. The current curve exhibits three characteristic regions. In a displacement interval $0 \geq \Delta z \geq -1.6 \text{ \AA}$ the current varies exponentially from ≈ 3 nA to ≈ 600 nA. Due to the exponential behaviour we denote this displacement interval the tunnelling region. Starting from $\Delta z \approx -1.6 \text{ \AA}$ we ob-

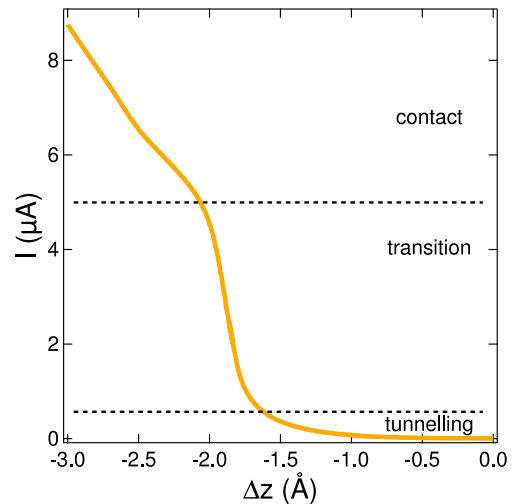


Fig. 5. Current-versus-displacement curve as acquired on the centre of a C_{60} molecule of the 5:6 type (see molecule encircled by a full line in Fig. 4). Zero displacement corresponds to initial tip height as fixed by opening the feedback loop at $V = 300$ mV and $I = 3$ nA. Decreasing displacements correspond to decreasing tip-molecule distances.

serve deviations from the exponential behaviour present in the tunnelling region: Within a displacement interval of $\approx 0.4 \text{ \AA}$ the current increases by a factor of eight to $\approx 5 \mu\text{A}$. In the tunnelling region, for comparison, a displacement change of 0.4 \AA would lead to a current change of only a factor of 3.5. We characterize this part of the current curve as the transition region which couples the tunnelling and the contact region, to be discussed next. In the contact region the current rises slowly with further approach of the tip towards the surface. Compared with the tunnelling region the current increase in the contact region is roughly a factor of four lower for a given displacement interval. Typically, when entering the contact regime, we observe conductances for the 5:6-type C_{60} in the range of $0.2\text{--}0.25G_0$ where $G_0 = 2e^2/h$ denotes the quantum of conductance. Although the current curve in the transition region appears to be continuous at the time resolution of the data acquisition, simulations [14] provide evidence that the transition region is characterized by fluctuations between configurations with or without the tip-molecule bond. The calculations reveal that only small energy differences discriminate between these configurations. By varying the effective temperature of the tip-molecule junction the width of the transition displacement interval can be modified. In particular, an effective temperature of 400 K must be assumed to model the experimentally observed width of the transition region. This temperature is reasonable in terms of an estimation of the maximum energy dissipation in the junction at the given voltage [22]. Two experimental results strongly corroborate this scenario of energy dissipation in the junction. First, the current noise in the transition region is significantly higher than in the tunnelling and the contact region [14]. This observation hints at an instability of the

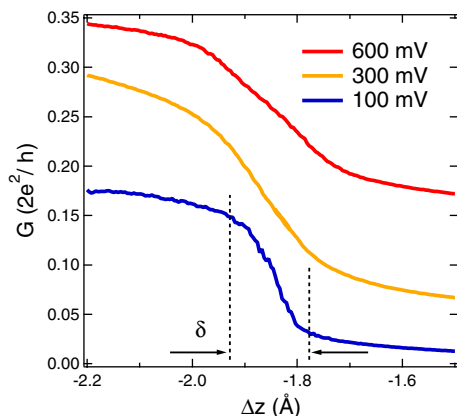


Fig. 6. Conductance-versus-displacement curves as acquired on a 5:6-type C_{60} molecule at the indicated voltage. The conductance is plotted in units of the quantum of conductance G_0 . For the conductance curve acquired at 100 mV (bottom curve) the width of the transition interval, δ , is indicated. Conductance curves acquired at 300 mV and 600 mV (middle and top curves, respectively) are vertically offset.

Table 1. Widths (δ) of the transition intervals of conductance curves acquired with the tip approaching the centre of a 5:6-type C_{60} molecule at different voltages (V) together with estimated effective temperatures T_{eff} of the molecule.

V (mV)	δ (Å)	T_{eff} (K)
100	0.2	300
300	0.4	400
600	0.5	700

tip-molecule distance in accordance with the fluctuation scenario. Second, the width of the transition range is dependent on the applied voltage. Figure 6 shows that the width δ of the transition region increases with increasing voltage applied to the junction (see also Tab. 1), consistent with increased heating at higher electron energies. According to the simulations introduced in reference [14] we estimate the molecule's effective temperatures at 100 mV and 600 mV as 300 K and 700 K, respectively.

4 Conclusions

Clusters fabricated from silver atoms on a silver surface reveal an unoccupied resonance whose energy shifts towards the Fermi level upon increasing the size of the assembly. The resonance is interpreted in terms of an atomic orbital broadened due to the interaction between the cluster and the supporting substrate surface. When approaching the tip towards a single C_{60} molecule the tip-molecule junction is stable up to currents as high as several μA . The

transition from tunnelling to contact is characterized by fluctuations of the tip-molecule distance induced by local heating of the junction.

We thank C. Cepek (Laboratorio Nazionale TASC, Italy) for providing C_{60} and the Deutsche Forschungsgemeinschaft for financial support through SPP 1153.

References

1. H.-V. Roy, P. Fayet, F. Patthey, W.-D. Schneider, B. Delley, C. Massobrio, *Phys. Rev. B* **49**, 5611 (1994)
2. N. Nilus, T.M. Wallis, W. Ho, *Science* **297**, 1853 (2002)
3. N. Nilus, T.M. Wallis, W. Ho, *Phys. Rev. Lett.* **90**, 046808 (2003)
4. J. Repp, G. Meyer, K.-H. Rieder, P. Hyldgaard, *Phys. Rev. Lett.* **91**, 206102 (2003)
5. S. Fölsch, P. Hyldgaard, R. Koch, K.H. Ploog, *Phys. Rev. Lett.* **92**, 056803 (2004)
6. J. Lagoute, X. Liu, S. Fölsch, *Phys. Rev. Lett.* **95**, 136801 (2005)
7. J.K. Gimzewski, R. Möller, *Phys. Rev. B* **36**, 1284 (1987)
8. J.I. Pascual, J. Méndez, J. Gómez-Herero, A.M. Baró, N. García, V.T. Binh, *Phys. Rev. Lett.* **71**, 1852 (1993)
9. L. Olesen, E. Lægsgaard, I. Stensgaard, F. Besenbacher, J. Schiøtz, P. Stoltze, K.W. Jacobsen, J.K. Nørskov, *Phys. Rev. Lett.* **72**, 2251 (1994)
10. A. Yazdani, D.M. Eigler, N.D. Lang, *Science* **272**, 1921 (1996)
11. L. Limot, J. Kröger, R. Berndt, A. Garcia-Lekue, W.A. Hofer, *Phys. Rev. Lett.* **94**, 126102 (2005)
12. N. Néel, J. Kröger, L. Limot, K. Palotas, W.A. Hofer, R. Berndt, *Phys. Rev. Lett.* **98**, 016801 (2007)
13. N. Néel, J. Kröger, L. Limot, R. Berndt, *Nanotechnology* **18**, 044027 (2007)
14. N. Néel, J. Kröger, L. Limot, T. Frederiksen, M. Brandbyge, R. Berndt, *Phys. Rev. Lett.* **98**, 065502 (2007)
15. L. Limot, J. Kröger, R. Berndt, A. Garcia-Lekue, W.A. Hofer, *Phys. Rev. Lett.* **94**, 126102 (2005)
16. L. Bürgi, O. Jeandupeux, A. Hirstein, H. Brune, K. Kern, *Phys. Rev. Lett.* **81**, 5370 (1998)
17. H. Jensen, J. Kröger, R. Berndt, S. Crampin, *Phys. Rev. B* **71**, 155417 (2005)
18. A. Bogicevic, P. Hyldgaard, G. Wahnström, B.I. Lundqvist, *Phys. Rev. Lett.* **81**, 172 (1998)
19. V.S. Stepanyuk, A.N. Klavysyuk, L. Niebergall, P. Bruno, *Phys. Rev. B* **72**, 153407 (2005)
20. M. Abel, A. Dmitriev, R. Fasel, N. Lin, J.V. Barth, K. Kern, *Phys. Rev. B* **67**, 245407 (2003)
21. X. Lu, M. Grobis, K.H. Khoo, S.G. Louie, M.F. Crommie, *Phys. Rev. Lett.* **90**, 096802 (2003)
22. M. Paulsson, T. Frederiksen, M. Brandbyge, *Nano Lett.* **6**, 258 (2006)